

COMMISSARIAT A L'ENERGIE ATOMIQUE

FR 900 3345

CENTRE D'ETUDES NUCLEAIRES DE SACLAY

CEA-CONF - -10080

Service de Documentation

F91191 GIF SUR YVETTE CEDEX

L1

A NEW THEORY OF COLLISIONS

GIRAUD B.G.

CEA Centre d'Etudes Nucleaires de Saclay, 91 - Gif-sur-Yvette (FR).  
Service de Physique Theorique

Communication présentée à : 6. International Conference on Recent Progress in  
Many Body Theories

Arad (IL)  
6-10 Nov 1989

CEA-IRF-CEN Saclay, BP 2, 91191 Gif/Yvette, France

Abstract: Instead of diagonalizing the many-body Hamiltonian  $H$ , we invert  $E-H$ , where  $E$  is a complex energy, eventually real. All the traditional approximations to diagonalization can be adjusted to inversion. We specially investigate mean-field methods. This lecture gives a scheme for the detailed proofs of our arguments, already published, and lists several numerically soluble cases where our new method has been successfully tested for the calculation of collision amplitudes.

### Introduction

Consider a system of  $N$  particles,  $N$  finite, large or small, with kinetic energies  $t_i$  and two-body interactions  $v_{ij}$ . An extraordinary amount of effort has been dedicated to the diagonalization of the corresponding Hamiltonian  $H=T+V$ . Among the most successful approximations, one may quote various brands of mean-field methods and their subsequent improvements: Hartree-Fock, BCS, shell model, etc. This effort has been able to provide many reliable approximations to the spectrum of  $H$ , whether  $N$  is large or small.

Much less effort has been dedicated to the calculation of the Green's function  $G=(E-H)^{-1}$ , whether  $E$  is real or complex. Such an inversion problem, however, is as interesting as the diagonalization, for the propagator  $G$  occurs as a key element of the theory in many practical problems. In particular, any collision theory sooner or later introduces  $G$  in the formalism...and the numerics.

This lecture is organized as follows. In Section 1, we show how any diagonalization approximation which is introduced according to the Rayleigh-Ritz variational principle can be adjusted into an inversion approximation, according to a Schwinger-like variational principle. In Section 2 we recall the results, already published, of a test of this approach for a trivially soluble, two-body problem. In Section 3, we recall the success also found for this method in the case of an exactly soluble

1. Inversion versus diagonalization

The well-known Rayleigh-Ritz variational functional reads

$$\mathcal{F} = \langle \Phi' | (H-E) | \Phi \rangle,$$

where  $\Phi', \Phi$  are infinitely flexible trial functions and  $E$  is a Lagrange multiplier. The stationarity of  $\mathcal{F}$  with respect to  $\Phi'$  (resp.  $\Phi$ ) induces the Schroedinger equation  $(H-E)\Phi=0$  (resp.  $\Phi'(H-E)=0$ ).

Whenever  $\Phi', \Phi$  are not infinitely flexible, one gets an approximation. For instance, if  $\Phi'$  and  $\Phi$  are products of single-particle orbitals  $\varphi'_i$  and  $\varphi_i$ , one obtains the Hartree approximation: the N-body Schroedinger equation is replaced by single-particle (but coupled) diagonalizations such as

$$(t_i + U_i - \eta_i) \varphi_i = 0, \tag{1.1}$$

where  $\eta_i$  and  $U_i$  are the well-known, self-consistent, Hartree self-energies and mean fields. (The most familiar form of  $U_i$  corresponds to the case when  $v$  is local, namely  $U(r) = \int dr' v(r-r') \sum_{j \neq i} \varphi_j^*(r') \varphi_j(r)$ , with the constraints  $\langle \varphi'_k | \varphi_l \rangle = \delta_{kl}$ .)

Naturally, these single-particle diagonalizations mean nothing but the conditions  $\delta \mathcal{F} / \delta \varphi'_i = 0$ . The point is, such single-particle, self-consistent diagonalizations can be performed numerically, and give a good approximation, while the full N-body diagonalization is impossible in practice.

We now investigate inversion. How can one calculate a matrix element  $D = \langle \chi' | G | \chi \rangle$ , where  $\chi'$  and  $\chi$  are arbitrary, square-integrable states? Answer: consider the functional

Stationarity of  $F$  with respect to  $\Phi'$  reads  $\Phi = G\chi$ , without any on-shell ambiguity if  $E$  is complex. Then it is easy to verify that the stationary value of  $F$  is the number under study, namely  $D$ . An identical result occurs for the stationarity with respect to  $\Phi$ , with  $\chi'G = \Phi'$ .

Whenever  $\Phi', \Phi$  are restricted, the approximation generated by  $F$  must be very similar to that generated by  $\mathcal{F}$ , since  $F$  and  $\mathcal{F}$  only differ via the "source terms"  $\langle \chi' | \Phi \rangle, \langle \Phi' | \chi \rangle$ .

In particular, let us assume that all four functions  $\chi', \chi, \Phi', \Phi$  are products of single particle orbitals  $\chi'_i, \chi_i, \Phi'_i, \Phi_i$ , respectively. Then the Hartree equations, Eqs.(1.1), are hardly modified: they become

$$(\eta_i - t_i - U_i)\Phi_i = \chi_i, \quad (1.2)$$

with a non-vanishing right-hand side which comes from the functional derivative  $\delta \langle \Phi' | \chi \rangle / \delta \Phi'_i$ . One clearly also gets a conjugate variational equation  $\chi'_i = \Phi'_i (\eta_i - t_i - U_i)$ .

As will be stressed over and over again in the following Sections, variational solutions for  $F$  are almost as easy to obtain as variational solutions for  $\mathcal{F}$ . Approximate methods for diagonalization can be extended to the calculation of the Green's function. For more technical details, including the case of identical particles, we refer the interested reader to refs.<sup>1)</sup>.

For the case of a calculation of a T-matrix amplitude, there is a slight complication of the theory, because the number under study reads  $\langle \chi' | V' G V | \chi \rangle$  rather than  $\langle \chi' | G | \chi \rangle$ . Here  $\chi$ , resp.  $\chi'$ , describe the initial, resp. final channel, and  $V$ , resp.  $V'$ , describe the corresponding channel potentials, namely the prior, resp. post interactions. These technicalities are dealt with in great detail in refs.<sup>1)</sup>. For the sake of simplicity, they will be omitted in the present lecture.

calculation of the T-matrix for such separable potential, two-body problems is trivial.

In particular, it is easy to calculate exactly the diagonal matrix element  $\mathcal{D} = \langle \chi | v | \chi \rangle + \langle \chi | v G v | \chi \rangle$ , with the following choice for  $\chi$ ,

$$\chi(q_1, q_2, k) = \pi^{-3} \beta^6 \exp\left[-\frac{\beta^2}{2} (q_1 - k)^2\right] \exp\left[-\frac{\beta^2}{2} (q_2 + k)^2\right]. \quad (2.1)$$

Here  $\chi$  describes particle 1 with momentum  $q_1$  in a wave packet with average momentum  $k$ , and particle 2 with momentum  $q_2$  in a wave packet with average momentum  $-k$ . The parameter  $\beta$  is obviously a width parameter. This wave packet representation for collisions is very convenient, for it allows calculations with square integrable states, without loss of generality or physical insight. This representation is again used systematically in the next Sections.

With this choice of  $\chi$ , it is easy to find that the exact calculation of  $\mathcal{D}$  reduces to Gaussian integrations and a numerical integration for a spectral function for S-waves. Then, for the variational approximation of  $\mathcal{D}$ , we choose the simplest possible ansatz: the trial functions  $\Phi, \Phi'$  introduced inside the functional  $F$  (or rather the modified functional which accounts for  $vGv$  instead of  $G$  alone) are also Gaussian wave packets. Namely we set

$$\Phi(q_1, q_2) = \chi(q_1, q_2, K),$$

according to Eq.(2.1). The only variational parameter is this average momentum  $K$ , and the functional becomes a function  $F(k, K)$ , according to the respective parameters of  $\chi$  and  $\Phi$ .

It is then trivial to choose  $K$  in order to cancel the derivative  $\partial F / \partial K$ , calculate the variational approximation to  $\mathcal{D}$ , and compare with the exact result. We have investigated many numerical ranges for all the parameters  $\lambda, v, \beta, \text{Im}E$ , etc.

While the exact result is unique, the variational approximation is

ref.<sup>2)</sup>.

In conclusion for this Section, the variational functional  $F$  is able, for a simple two-body soluble case, to provide a satisfactory  $G$ - (or  $T$ -) matrix element with just one variational parameter. It is not even necessary to use a full single-particle orbital as a variational tool, and the use of Eqs.(1.2) can be spared for more elaborate cases. Such cases are the subject of Sections 3 and 4.

### 3. A three-body soluble example

We briefly recall here the results of ref.<sup>3)</sup>. Our model is an extension of the model of Section 2. With three particles, there are now three separable potentials  $v_{ij}(q_{ij}, q')$ , analogous to the potential  $v$  used in Section 2. The channel wave packet  $\chi$  is the simplest possible generalization of Eq.(2.1), namely a product of three single-particle Gaussians, boosted by  $k_1, k_2, k_3$  respectively, with the constraint  $k_1 + k_2 + k_3 = 0$ .

The exact matrix element  $D = \langle \chi | G | \chi \rangle$  is obtained as  $D = \langle \chi | \Psi \rangle$ , with  $\Psi = G\chi$ , hence  $(E - T - v_{12} - v_{13} - v_{23})\Psi = \chi$ , then  $\Psi = G_0\chi + \Psi_1 + \Psi_2 + \Psi_3$ , with  $G_0 = (E - H_0)^{-1}$ ,  $\Psi_1 = G_0 v_{23}\Psi$ ,  $\Psi_2 = G_0 v_{13}\Psi$ ,  $\Psi_3 = G_0 v_{12}\Psi$ . As usual in manipulations leading to Faddeev-type equations, this leads to three coupled equations for  $\Psi_1, \Psi_2, \Psi_3$ . These can be easily solved numerically, for the separability of  $v$  induces separability for each component  $\Psi_i$  of  $\Psi$ . Numerical results are shown on Fig.2, for one of the many sets of parameters we have investigated. More details are available in ref.<sup>3)</sup>.

The mean field approximation is obtained by brute force solution of Eqs.(1.2). The separability of  $v$  makes the Hartree mean field very simple. The corresponding estimate for  $\langle \chi | G | \chi \rangle$  is shown on Fig.3 for the same set of parameters as for Fig.2. There is little need to comment on the good agreement between the exact and the approximate amplitudes. Notice however the wrong sign of  $\text{Re}D$  for large, negative  $\lambda$ .

#### 4. A four-body soluble example

In ref.<sup>4)</sup> the potential  $v$  is now taken as "super separable", namely, in momentum representation,

$$\langle q'_i q'_j | v_{ij} | q_i q_j \rangle = -\lambda f(q'_i) f(q'_j) f(q_i) f(q_j),$$

where  $f$  is any suitable form factor (actually a Lorentzian in our numerical application). This differs from the potential of Sections 2 and 3, where  $v$  was a function of just the relative momenta, such as  $q_{ij} = (q_i - q_j)/2$ .

We are again interested in the diagonal matrix element  $D = \langle \chi | G | \chi \rangle$ , where  $\chi$  is now a product of four boosted wave packets,

$$\chi(q_1, \dots, q_4) = \Gamma(q_1 - k) \Gamma(q_2 - k) \Gamma(q_3 + k) \Gamma(q_4 + k).$$

With this choice for  $\chi$ , many symmetries between the four particles are transparent and greatly help the solubility of the model. The single-particle wave-packets  $\Gamma$  are chosen as one-dimensional and Lorentzian, hence many integrations reduce to contour integrations.

The algebraic manipulations which convert the exact inversion problem  $\Psi = G\chi$  into a soluble set of coupled integrodifferential equations for the various components of  $\Psi$  cannot be detailed here. They are obviously greatly simplified by the "super separability" of  $v$ . All details can be found in ref.<sup>4)</sup>. Here we rather indicate how the mean-field equations are easy to solve:

The main simplification comes from the mean-field potential. Because of the symmetries between all four particles and the scalar nature of  $v$ , it does not depend on the label  $i$  and reads

$$\langle q' | U | q \rangle = -3 \lambda f(q') f(q) \alpha^2 n^{-1}, \text{ with } \alpha = \langle f | \varphi_1 \rangle \text{ and } n = \langle \varphi_1^* | \varphi_1 \rangle.$$

in terms of three parameters only,  $\eta$ ,  $\alpha$  and  $n$ ,

$$\varphi_1(q) = (\eta - q^2)^{-1} [ \Gamma(q-k) - 3 \lambda \alpha^3 n^{-1} f(q) ].$$

All practical calculations amount to the search for the self-consistency of  $\eta$ ,  $\alpha$  and  $n$ . The results of ref.<sup>4)</sup> are illustrated by Fig.4, where the agreement between exact and mean-field amplitudes, for at least several ranges of parameters, is striking.

We have thus found a four-body case where a mean-field estimate of the Green's function is a good approximation.

#### 5. The kinetic energy model

While the diagonalization of  $T = \sum_{i=1}^N t_i$  is trivial, the calculation of a matrix element  $\langle \chi | (E-T)^{-1} | \chi \rangle$  still requires an intractable multiple dimension integral when  $N$  is large. Hence our "mean-field" approach deserves investigation. We recall now the results of ref.<sup>5)</sup>.

Set  $\chi$  as a product  $\chi(q_1, \dots, q_N) = \Gamma(q_1 - k_1) \dots \Gamma(q_N - k_N)$ , with a rotation and/or parity degeneracy between the boosts  $k_i$ . For obvious symmetry reasons, it is then sufficient to solve only one among Eqs.(1.2), for instance

$$(\eta - q^2) \varphi_1(q) = \Gamma(q - k_1), \text{ with } \eta = E - (N-1)\theta \text{ and } \theta = \frac{\langle \varphi_1^* | t | \varphi_1 \rangle}{\langle \varphi_1^* | \varphi_1 \rangle}.$$

Hence in momentum representation  $\varphi_1 = (\eta - t)^{-1} \Gamma_1$  is known, except for the self-consistency of  $\eta$  (or  $\theta$ ).

As shown in ref.<sup>5)</sup>, this self-consistency condition can be framed into the cancellation of a polynomial, which makes the model highly analytical. A careful analysis of the solutions shows an extremely interesting result: when  $E$  is real, there exists a pair of solutions  $\eta, \eta^*$  with finite imaginary parts (even though  $\text{Im}E=0$ ). One of these solutions



numerical cases investigated, this approximation is reliable in a wide range of energies.

## 6. The case of a semi-realistic potential

The confidence grown from the soluble examples described in Sections 2-5 justifies solving Eqs.(1.2) in a case where there is no exact solution for comparison. Only the consistency of the approximate results will be available for a criticism of the method.

Fig.6 is taken from ref.<sup>6)</sup>, which is a brute force, Hartree calculation of elastic proton-triton scattering. The nuclear interaction is taken as semi-realistic, namely a local, two-body Gaussian. Particle label 1 refer to projectile-like orbitals, labels 2-4 refer to target-like orbitals. There is complete symmetry between orbitals 2-4, hence labels 3 and 4 are omitted.

The Figure corresponds to final momentum at 90° (along y) away from initial momentum (along z). The plots are momentum density plots of the variational orbitals  $\varphi, \varphi'$  (which make the trial functions  $\Phi, \Phi'$ ) in the reaction plane (z y).

Not surprisingly, target orbitals  $\varphi_2, \varphi'_2$ , which carry less momentum than the projectile orbitals  $\varphi_1, \varphi'_1$ , are more centered and less deformed. It is also satisfactory that the density center of  $\varphi_1$  lies "forward", while the density center of  $\varphi'_1$  lies in the "tranverse" direction. In so far as  $\Phi, \Phi'$  represent intermediate states of the collision, the Figure gives a picture of the reaction mechanism.

This Figure is only part of a whole atlas, corresponding to various energies, scattering angles, etc. At present, the numerical evidence favors a smooth behavior of the variational solution as a function of its control parameters.

To conclude this Section, we seem to have a semi-realistic case where

The guess of good trial functions has been for decades at the core of the theory of nuclear, atomic and molecular spectra. An exactly similar approach is available for the theory of propagators. One just has to slightly change the variational principle which underlies the theory.

Naturally, many auxilliary, but important questions must be investigated while solving our "extended" Hartree(-Fock, -Bogoliubov, -etc.) equations. In particular one should understand the multiplicity of solutions, their stability, the rôle of boundary conditions. This program will likely request some empiricism before all the problems are fully understood. But the same difficulty was met for a complete justification of the shell model. Our approach to propagators is not just formal, but generates numbers which can be compared with experimental data.

It is a pleasure to thank the organizers of this conference for their invitation and the opportunity of this lecture.

long-dashed line represents a linear superposition of "1" and "2".

Figs. 2 and 3: Three-body case, separable potential. Good agreement between the exact amplitude (Fig.2, top) and its mean-field approximation (Fig.3, bottom), except for  $\text{Re } D$  with large, negative coupling constants.

Fig. 4: Four-body case, super-separable potential. Agreement between the exact and the mean-field amplitudes, as functions of the coupling constant.

Fig. 5: Kinetic energy model. Agreement between the exact ( $E_x$ ) and the mean-field ( $A_p$ ) matrix elements of the free Green's function, as functions of the real part of the energy.

Fig.6: Momentum density patterns of the trial orbitals  $\varphi, \varphi'$  for an elastic p-t scattering at  $90^\circ$ . Notice how  $\varphi_1$  concentrates in the forward, z-direction, while  $\varphi'$  concentrates in the tranverse, y-direction. Notice also how both orbitals show a "horn" at  $45^\circ$ , which is essential for a non-vanishing overlap between these orbitals.

#### REFERENCES

- 1) B.G.Giraud, M.A.Nagarajan and I.J.Thomson, Ann.Phys.(NY) 152, 475 (1984)  
B.G.Giraud, M.A.Nagarajan and C.J.Noble, Phys.Rev.A 34, 1034 (1986)
- 2) M.A.Nagarajan and B.G.Giraud, Phys.Rev.C 27, 232 (1983)
- 3) Y.Abe and B.G.Giraud, Nucl.Phys. A440, 311 (1985)
- 4) Joerg Lemm, Diplomarbeit (1989), Institut fuer Theoretische Physik, Universitaet Muenster, FRG
- 5) B.G.Giraud, Physica 19D, 112 (1986)
- 6) B.G.Giraud and M.A.Nagarajan, Saclay preprint SPh-T 88/89, submitted to Phys.Rev.C

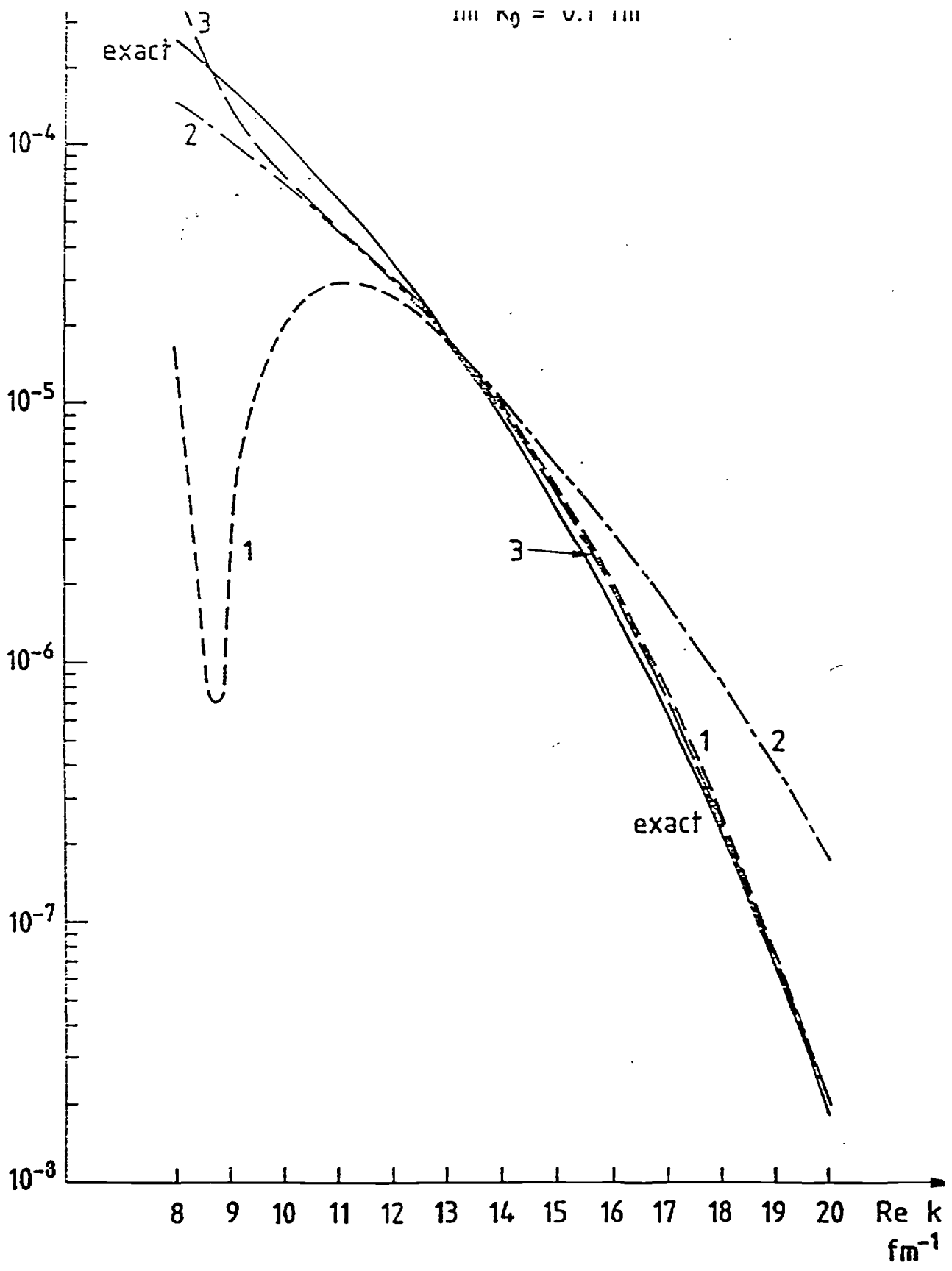


Fig. 1

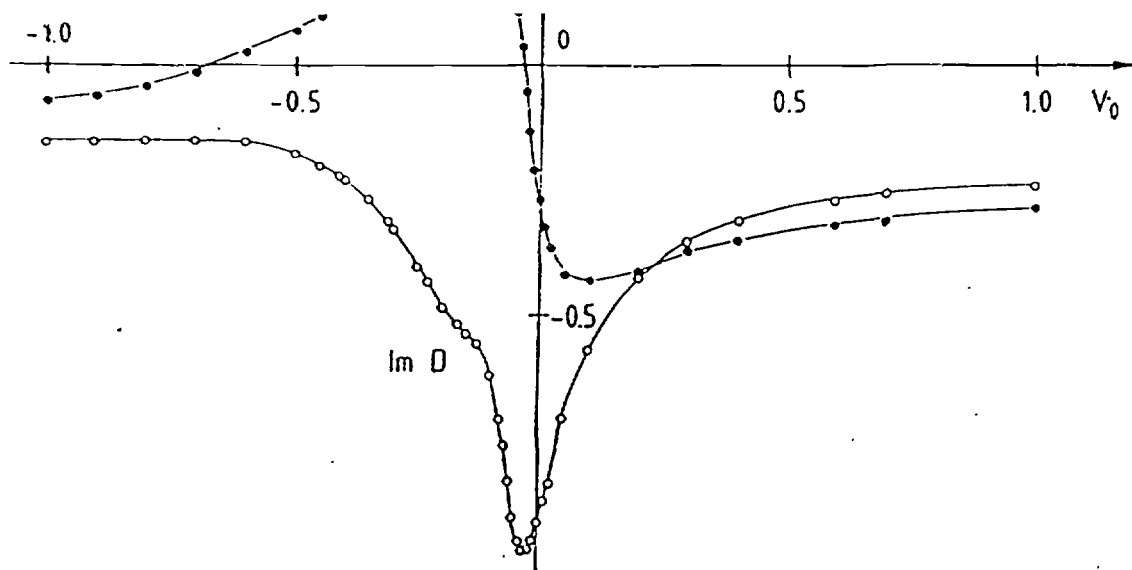
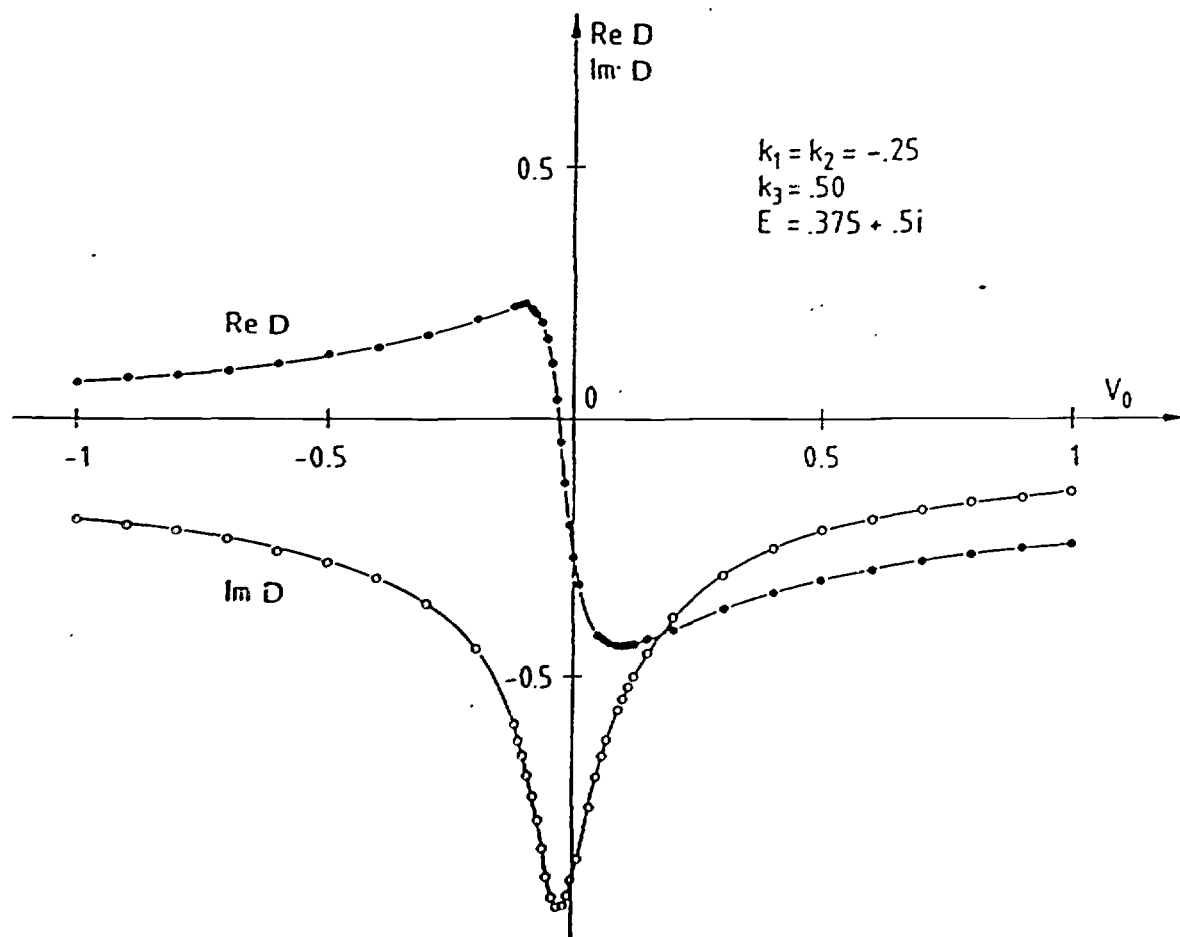


Fig. 2 Exact multistep amplitude as a function of the strength. Compare with fig. 3



3 Real and imaginary parts of the mean-field, multistep amplitude  $D$  as a function of the interaction strength  $V_0$ .

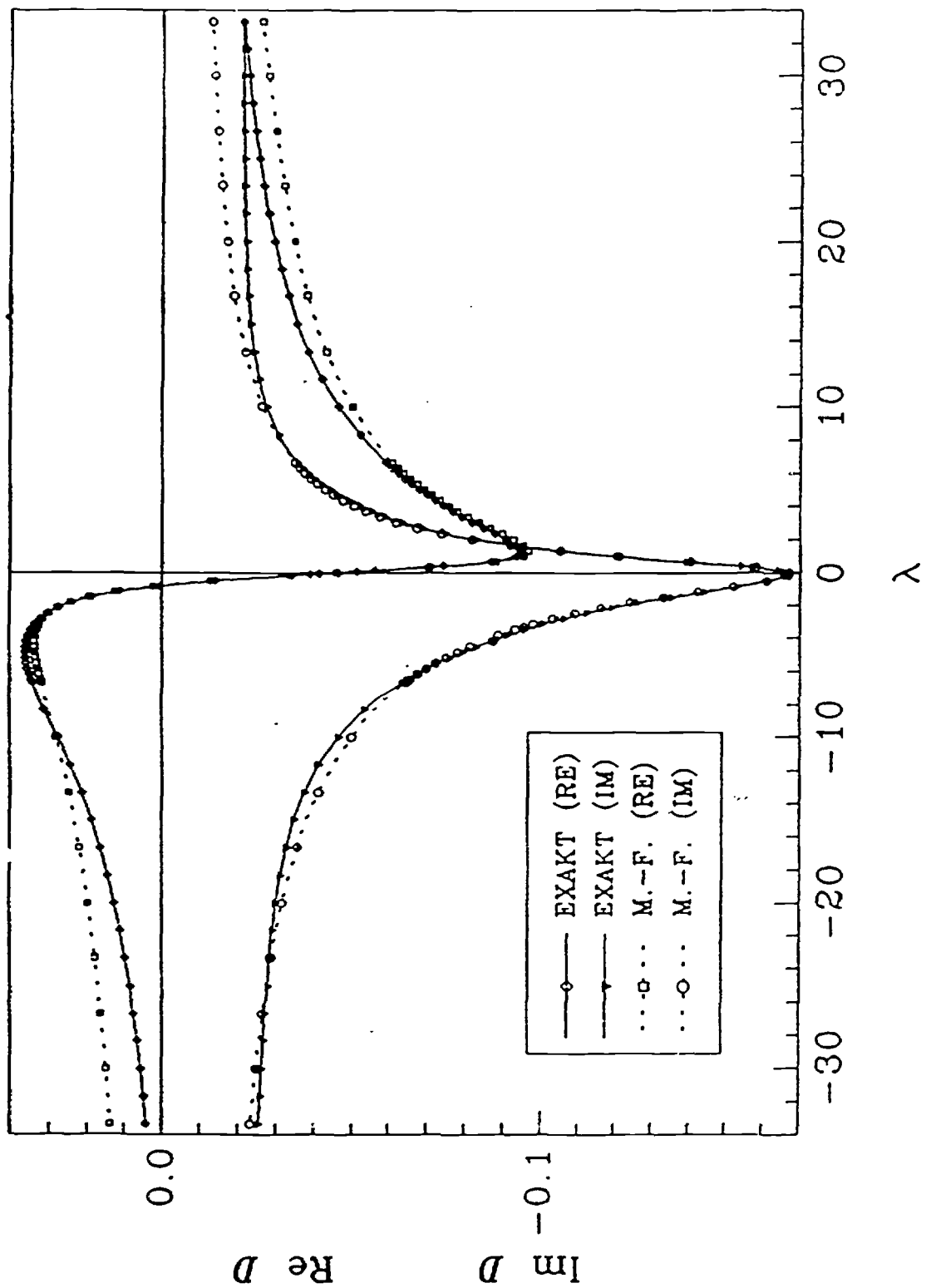


Abbildung 4.1: Der Vergleich für die Diagonalamplitude  $D$  zwischen exakter und Mean-Field-Rechnung (M.-F.) bei  $K = 1$  und  $\epsilon = 4$ .

Fig. 4

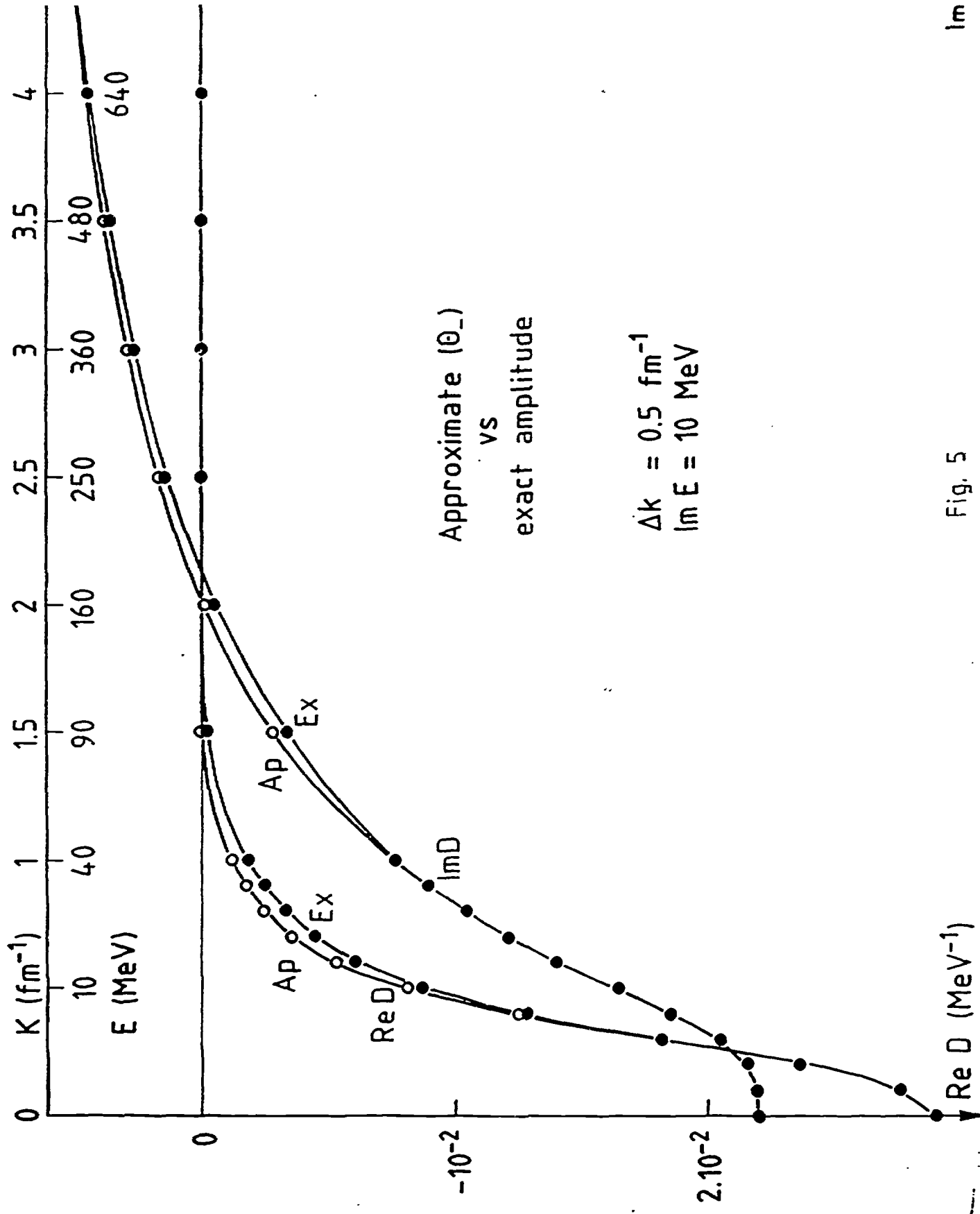


Fig. 5

Im

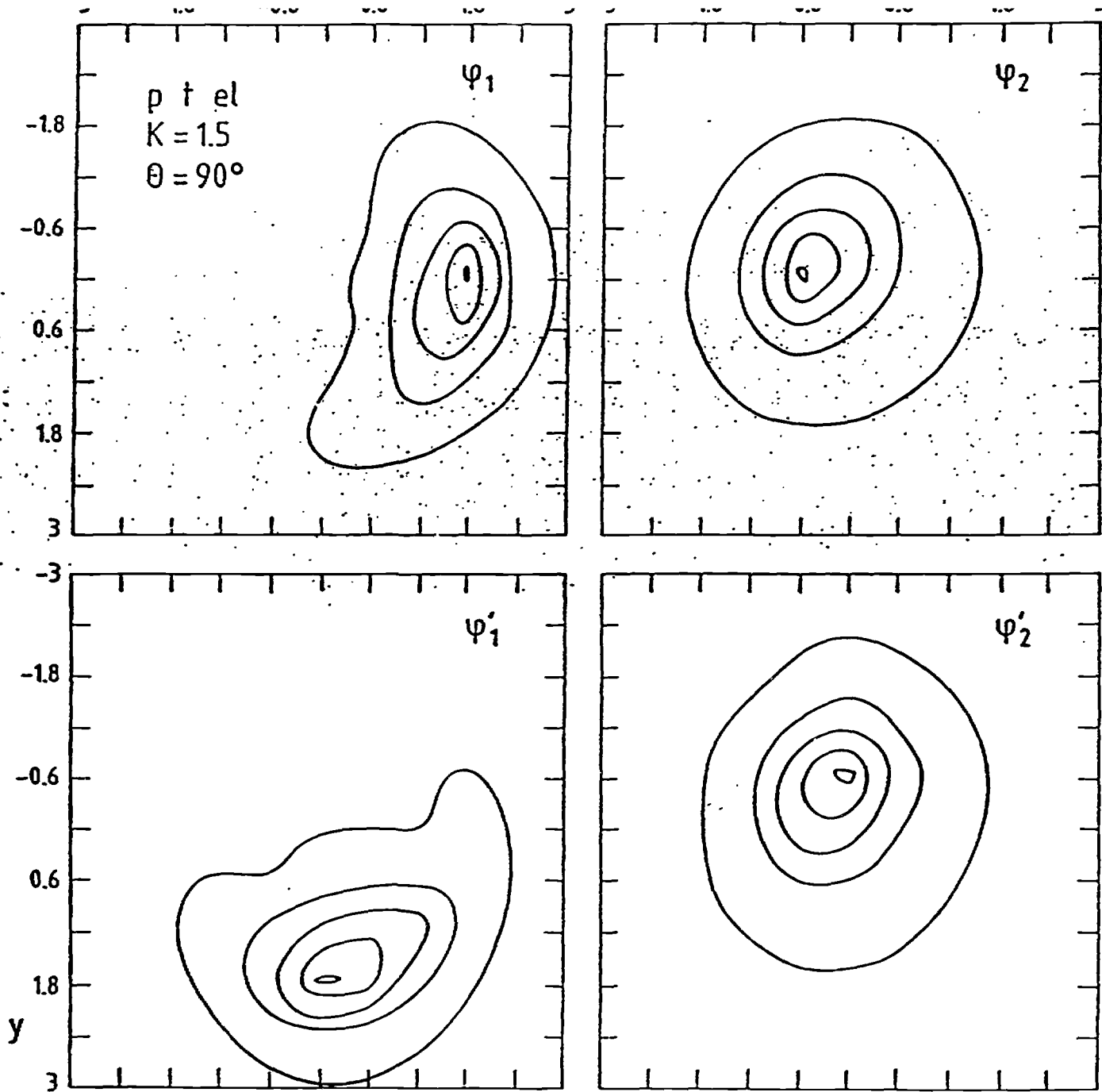


Fig. 6